

## BVRI SURFACE PHOTOMETRY OF MIXED MORPHOLOGY PAIRS OF GALAXIES. III. THE THIRD DATA SET

A. Franco-Balderas, H. M. Hernández-Toledo, D. Dultzin-Hacyan, and M. Rosado

Instituto de Astronomía  
Universidad Nacional Autónoma de México, México

*Received 2005 February 9; accepted 2005 June 30*

### RESUMEN

Este es el tercero de una serie de artículos dedicados al estudio de las propiedades fotométricas de galaxias elípticas y espirales en pares interactuantes. Presentamos las magnitudes totales (*BVRI*), así como también los correspondientes perfiles geométricos ( $\epsilon = 1 - b/a$ , PA y  $a_4/a$ ), de color y de brillo superficial para un conjunto de 10 pares de morfología mixta (E/S0+S) pertenecientes al Catálogo de Pares de Galaxias Aisladas de Karachentsev (KPG). Para la mayor parte de los objetos aquí presentados, hemos determinado por primera vez los parámetros fotométricos. La información obtenida de la fotometría superficial, en combinación con imágenes procesadas y diagramas de color, ha resultado muy útil para probar y reevaluar la clasificación morfológica de las galaxias en cada par. En la presente muestra encontramos 5 pares (E+S) verdaderos, 4 sistemas lenticular-espiral (S0+S) y un par espiral-espiral (S+S). No encontramos evidencia clara en favor del efecto Holmberg en nuestro conjunto de pares mixtos. La existencia de un gran número de pares (E+S) aislados ( $\sim 50\%$  en nuestra muestra), introduce interesantes preguntas para los modelos de formación de galaxias.

### ABSTRACT

This is the third of a series of papers devoted to the study of the photometric properties of spiral and elliptical galaxies in interacting pairs. We report broad band (*BVRI*) total magnitudes, as well as surface brightness, color and geometric ( $\epsilon = 1 - b/a$ , PA and  $a_4/a$ ) profiles for a sample of 10 mixed morphology (E/S0+S) pairs drawn from the Karachentsev Catalogue of Isolate Pairs of Galaxies (KPG). Most of the objects reported here have their photometric parameters derived for the first time. Surface photometry in combination with image processing and color diagrams are useful to test and reevaluate the morphological classification of each galaxy in these pairs. We find 5 true (E+S) pairs in the present sample, 4 lenticular-spiral (S0+S) systems and 1 spiral-spiral (S+S) pair. We found no clear evidence of a Holmberg effect in our sample of mixed pairs. The existence of a large number of isolated (E+S) pairs ( $\sim 50\%$  in our sample) rises interesting questions for models of galaxy formation.

**Key Words:** GALAXIES: ELLIPTICAL — GALAXIES: FUNDAMENTAL PARAMETERS — GALAXIES: INTERACTIONS — GALAXIES: PHOTOMETRY — GALAXIES: SPIRAL — GALAXIES: STRUCTURE

### 1. INTRODUCTION

Large area surveys are recently enabling studies of large samples of interacting galaxies. This is expanding our ideas about interaction stimulation of multiwavelength emission from galaxies and is giving

us new insights into the phenomenology and physics of interactions. However, to fully quantify the processes involved, a complementary approach entails obtaining deeper and higher resolution observations of carefully selected samples of interacting galaxies to provide statistically significant local templates

TABLE 1  
JOURNAL OF OBSERVATIONS

Galaxy Pair	$T_B$ (s)	$< B >_{\text{FWHM}}$ (")	$T_V$ (s)	$< V >_{\text{FWHM}}$ (")	$T_R$ (s)	$< R >_{\text{FWHM}}$ (")	$T_I$ (s)	$< I >_{\text{FWHM}}$ (")	Scale ("/pixel)
KPG339	2×1800	1.8	2×1200	1.9	2×420	1.9	2×240	1.8	0.51
KPG353	2× 720	2.3	3× 240	2.4	3× 80	2.3	3× 40	2.2	0.79
KPG393	2×1800	1.5	2×1200	1.6	3×360	1.4	3×120	1.6	0.51
KPG394	2× 600	1.9	2× 600	1.9	3×240	2.1	3×240	2.1	0.79
KPG408	2×2100	2.3	3× 480	1.8	3×180	2.3	3×120	2.3	0.51
KPG445	2×1800	2.2	3× 600	1.8	3×240	2.4	3×150	2.4	0.51
KPG491	2×2400	1.4	2×1200	1.4	3×300	1.4	3×150	1.3	0.51
KPG526	2×2000	2.8	2× 330	2.7	3×150	2.4	3× 80	2.1	0.51
KPG548	2×2400	2.0	2× 520	1.9	3×240	1.9	3× 90	1.5	0.51
KPG553	2×1800	1.5	3× 480	1.7	3×200	1.4	3×100	1.4	0.51

that will be effective in helping us evaluate results of deep and high-redshift surveys.

Isolated binary galaxies composed of a gas-poor early-type and a gas-rich late-type (the so called mixed morphology (E/S0+S) pairs) occupy a special place among physical pairs. Not only can they represent a possible transition stage toward the coalescence of a compact group (Rampazzo & Sulentic 1992; Wiren et al. 1996) but they certainly represent the best local laboratory from which to study secular evolutionary processes due to interactions, from induced star formation episodes to AGN stimulation by gas cross-fuelling (Domingue et al. 2003; Franco-Balderas et al. 2003 (Paper I); Franco-Balderas, Hernández-Toledo, & Dultzin-Hacyan 2004 (Paper II)). A large population of isolated mixed pairs is now known (e.g., Catalogue of Isolated Pairs of Galaxies in the Northern Hemisphere, Karachentsev 1972) and its southern extension Reduzzi & Rampazzo 1996).

Isolated mixed pairs represent a non-cluster sample where the fraction of ellipticals is unusually high for low density environments. Mixed pairs also provide a unique vantage point on the interaction-activity connection. There is a single gas rich component in each pair which somewhat reduces the ambiguity in the interpretation of imaging and spectroscopic data. Evidence for an evolutionary link between groups and binary galaxies has been found both from numerical simulations and observations.

N-body numerical simulations of isolated groups indicate that dynamical friction should play an important role in the evolution of groups (Athanasoulas, Makino, & Bosma 1997). In such a scenario

TABLE 2  
EXTINCTION AND CALIBRATION  
COEFFICIENTS FOR THE OPTICAL  
OBSERVATIONS

Extinction Coefficients		
	April 2000	June 2000
$k_b$	$0.273 \pm 0.052$	$0.204 \pm 0.022$
$k_v$	$0.176 \pm 0.045$	$0.125 \pm 0.021$
$k_r$	$0.121 \pm 0.042$	$0.072 \pm 0.022$
$k_i$	$0.083 \pm 0.044$	$0.049 \pm 0.027$
Calibration Coefficients		
$\alpha_o$	$2.456 \pm 0.040$	$1.576 \pm 0.006$
$\alpha_1$	$0.014 \pm 0.067$	$0.012 \pm 0.008$
$\beta_o$	$0.487 \pm 0.003$	$0.786 \pm 0.011$
$\beta_1$	$0.895 \pm 0.006$	$0.803 \pm 0.014$
$\epsilon_o$	$0.170 \pm 0.004$	$0.282 \pm 0.018$
$\epsilon_1$	$1.068 \pm 0.012$	$1.009 \pm 0.040$
$\gamma_o$	$-0.092 \pm 0.016$	$0.044 \pm 0.013$
$\gamma_1$	$1.063 \pm 0.023$	$1.090 \pm 0.015$

the groups are not in dynamical equilibrium because of the high frequency of galaxy interactions. Wiren et al. (1996) have constructed theoretical models for samples of close pairs by assuming that initially the galaxies were members of small groups which degenerate to binary systems via mergers. A common belief is that early-type (E/S0) galaxies are formed by merging of spiral galaxies (Barnes & Hernquist 1992; Mihos 1995).

TABLE 3  
GENERAL (NED) DATA FOR THE OBSERVED GALAXIES

KPG Number	Identif.	$B$ mag	$x_{1-2}$ (')	$x_{1-2}$ (kpc)	$V_{rad}$ (km s <sup>-1</sup> )	$\sigma_0$ (km s <sup>-1</sup> )	$V_{max}$ (km s <sup>-1</sup> )	$A_{25}$ (kpc)
KPG339A	NGC 4446	14.56	1.57	43.6	7316 ± 9	...	...	29.3
KPG339B	NGC 4447	14.90	...	...	7203 ± 20	...	...	23.2
KPG353A	Arp116 (01)	12.06	2.57	12.7	1422 ± 4	102 ± 27	...	14.7
KPG353B	Arp116 (02)	9.66	...	...	1117 ± 6	334 ± 10	87 ± 10	29.6
KPG393A	PGC048702	15.60	2.38	74.5	8015 ± 38	...	...	22.3
KPG393B	PGC048724	15.42	...	...	7991 ± 26	...	...	31.9
KPG394A	NGC 5296	14.89	1.57	15.4	2244 ± 2	218 ± 14	50 ± 20	8.7
KPG394B	NGC 5297	12.29	...	...	2409 ± 2	165 ± 66	...	43.5
KPG408A	IC 0970	15.10	1.12	16.8	4064 ± 27	193 ± 10	...	17.2
KPG408B	PGC050014	15.29	...	...	4012 ± 21	...	...	11.8
KPG445A	NGC 5782	14.59	0.87	31.4	9652 ± 44	374 ± 14	...	58.1
KPG445B	PGC053382	14.48	...	...	8829 ± 52	...	...	21.8
KPG491A	PGC057617	15.70	1.25	49.8	10183 ± 70	...	...	31.0
KPG491B	IC 1206	14.50	...	...	10123 ± 10	...	...	50.0
KPG526A	NGC 6500	13.05	2.31	27.7	3003 ± 5	214 ± 6	...	25.3
KPG526B	NGC 6501	13.03	...	...	3068 ± 11	238 ± 27	...	21.4
KPG548A	NGC 6962	12.99	1.76	28.8	4211 ± 6	272 ± 35	150 ± 20	54.8
KPG548B	NGC 6964	13.72	...	...	3804 ± 16	284 ± 47	...	26.5
KPG553A	PGC066170	14.90	1.42	28.6	4826 ± 22	...	...	32.6
KPG553B	PGC066178	15.18	...	...	5025 ± 20	...	...	19.9

On the other hand, the observational work, especially that on mixed morphology (E/S0+S) binary galaxies (Rampazzo & Sulentic 1992) seems to support this, namely: (i) ellipticals that could be merger products, implying that some (E+S) pairs are transient stages in the collapse of higher order systems (Teerikorpi 2001) and (ii) false spirals with interaction-induced arms implying that some lenticular galaxies develop arms or arm-like features as a result of close interaction with a neighbor: S0 misclassified as spirals in both early-type and late-type pairs. That is, interactions and merging of galaxies play an important role in the evolution of galaxy morphology (Schweizer & Seitzer 1992).

With these evidences in mind, Franco-Balderas et al. (2003; 2004) have presented deep multicolor broad band (BVRI) photometry for two sets of 11 and 10 mixed pairs respectively from the KPG catalog finding an important number of true (E+S) pairs (10/21).

In the present paper, we continue analyzing the photometric and morphological properties of a third

set of 10 mixed pair candidates from the original KPG catalogue with the aim to define the largest possible subset of true (E+S) pairs for more detailed studies of their structural parameters and the implications for their evolution in non-isolated environments.

We present  $B$ ,  $V$ ,  $R$ , and  $I$  photometric data: total magnitudes,  $(B - V)$ ,  $(B - R)$ ,  $(B - I)$  colors, surface brightness profiles, color profiles and geometric ( $\epsilon = 1 - b/a$ , PA and  $a_4/a$ ) profiles with emphasis on the morphology and its relation to the global photometric properties.

## 2. OBSERVATIONS AND DATA REDUCTION

The observations of the third set of mixed pairs were carried out on April and June 2000 at Observatorio Astronómico Nacional (OAN)<sup>1</sup>. The CCD BVRI photometry (in the Johnson-Cousins system) was obtained with a SITE1 CCD detector attached

<sup>1</sup>San Pedro Mártir, Baja California, México, operated by the Instituto de Astronomía, Universidad Nacional Autónoma de México (IA-UNAM).

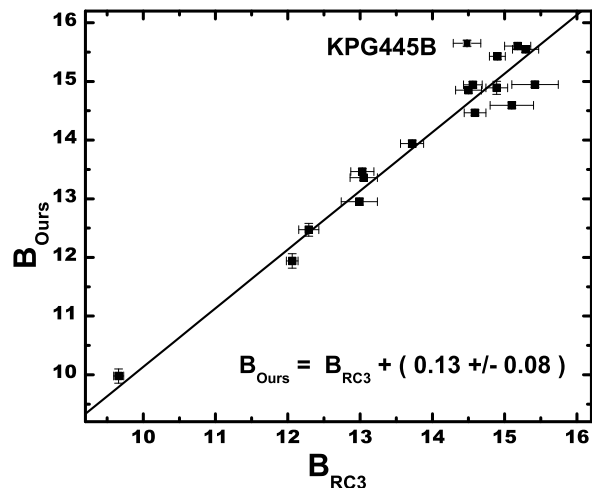


Fig. 1. Comparison between our total  $B$  magnitudes and total magnitudes from RC3 Catalogue.

to the 0.84 m and 1.5 m telescopes, covering an area of about  $6.7' \times 6.7'$  and  $4.3' \times 4.3'$ , respectively. Table 1 indicates the image scale in  $''/\text{pixel}$ .

We have applied no special strategy in selecting this third subset of mixed pairs. Available observing time and weather conditions were the main factors limiting the number of observed pairs. A journal of this third set of the photometric observations is given in Table 1. Column 1 gives the original catalogue number, Columns 2 to 9 give the number of frames per filter, the integration time (in seconds) and seeing conditions (in  $''$ ).

Images were debiased, trimmed, and flat-fielded using standard IRAF<sup>2</sup> procedures.

Photometric calibration was achieved by nightly observations of standard stars of known magnitudes from the Landolt lists (Landolt 1992). Standard stars with a color range  $-0.29 \leq (B - V) \leq 1.07$  and  $-0.30 \leq (V - I) \leq 1.11$  were observed. The main extinction and calibration coefficients of transformation to the standard system (see Paper II), can be found in Table 2.

Table 3 gives some relevant information for the observed pairs from the literature. Column 1 is the KPG catalogue number, Columns 2 and 3 report other identifications and the apparent  $B$  magnitude from NED, Column 4 is the projected separation of each pair in arc-minutes, and Column 5 is the linear

<sup>2</sup>The IRAF package is written and supported by the IRAF programming group at the National Optical Astronomy Observatories (NOAO) in Tucson, Arizona. NOAO is operated by the Association of Universities for Research in Astronomy (AURA), Inc. under cooperative agreement with the National Science Foundation (NSF).

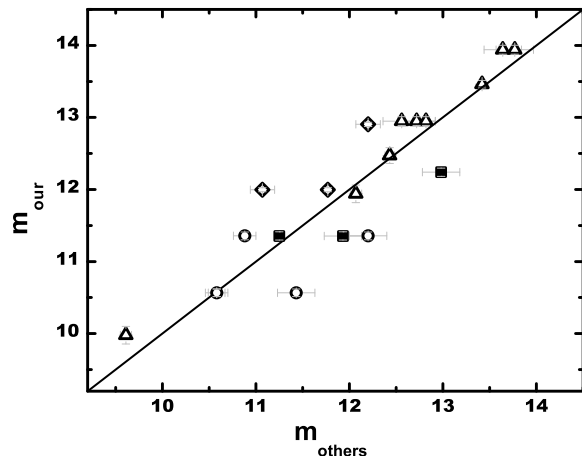


Fig. 2. Comparison between our total  $BVRI$  magnitudes and the corresponding ones from other authors:  $B$ -band (triangles),  $V$ -band (diamonds),  $R$ -band (squares), and  $I$ -band (circles).

separation in kpc, Column 6 the radial velocity for each component in  $\text{km s}^{-1}$  from NED, Columns 6 and 7 report the central velocity dispersion and the maximum velocity of rotation along the major axis in  $\text{km s}^{-1}$  from LEDA. Finally, Column 9 gives the major axis diameter, at  $\mu_B = 25 \text{ mag}''$ , in kpc ( $H_0 = 75 \text{ km s}^{-1} \text{ Mpc}^{-1}$ ).

Total magnitudes were computed alternatively using polygonal apertures within POLYPHOT routines in IRAF. Foreground stars within the aperture were removed interactively. Elliptical surface brightness contours were fit using the STSDAS package ISOPHOTE in IRAF. Typical errors for the geometric parameters are  $\Delta\epsilon = 0.05$ ,  $\Delta PA = 7^\circ$ , and  $\Delta(a_4/a) * 100 = 0.0007$ . Our derived parameters are generally in good agreement with those reported in the literature. For more details concerning these procedures see Paper I and II.

### 2.1. Standard Stars

A comparison of our CCD magnitudes against those reported in Landolt (1992) for 11 stars in common shows no significant deviations. The internal errors can be described by a  $\sigma_B \sim 0.029$ ,  $\sigma_V \sim 0.027$ ,  $\sigma_R \sim 0.028$  and  $\sigma_I \sim 0.030$ .

### 2.2. Paired Galaxies

The total typical uncertainties in  $B$ ,  $V$ ,  $R$ , and  $I$  bands are 0.11, 0.07, 0.10 and 0.10 for the April run and 0.06, 0.03, 0.06, and 0.05 for June run, respectively. However, see Table 4 for individual uncertainties.



TABLE 4  
OBSERVED MAGNITUDES

KPG	<i>B</i>	<i>V</i>	<i>R</i>	<i>I</i>	( <i>B</i> − <i>V</i> )	Notes
KPG339A	14.94 ± 0.06	14.39 ± 0.03	13.89 ± 0.05	13.12 ± 0.05	0.55 ± 0.07	...
KPG339B	15.43 ± 0.06	14.42 ± 0.03	13.79 ± 0.06	13.09 ± 0.05	1.01 ± 0.08	...
KPG353A	11.94 ± 0.12	11.26 ± 0.07	10.76 ± 0.10	10.11 ± 0.11	0.68 ± 0.14	...
KPG353B	9.98 ± 0.12	9.03 ± 0.07	8.43 ± 0.11	7.62 ± 0.11	0.95 ± 0.13	...
KPG393A	15.43 ± 0.05	14.57 ± 0.02	13.92 ± 0.05	12.98 ± 0.05	0.86 ± 0.05	...
KPG393B	14.95 ± 0.05	14.29 ± 0.02	13.74 ± 0.05	13.08 ± 0.05	0.66 ± 0.06	...
KPG394A	14.89 ± 0.11	14.22 ± 0.07	13.69 ± 0.10	12.80 ± 0.10	0.67 ± 0.13	...
KPG394B	12.47 ± 0.11	11.84 ± 0.07	11.30 ± 0.10	10.57 ± 0.10	0.63 ± 0.12	BS <sup>a</sup>
KPG408A	14.60 ± 0.05	13.62 ± 0.02	13.00 ± 0.05	12.32 ± 0.05	0.98 ± 0.05	BS <sup>a</sup>
KPG408B	15.55 ± 0.05	14.94 ± 0.02	14.54 ± 0.05	14.01 ± 0.05	0.61 ± 0.06	BS <sup>a</sup>
KPG445A	14.47 ± 0.05	13.43 ± 0.02	12.77 ± 0.05	11.93 ± 0.05	1.04 ± 0.05	BS <sup>a</sup>
KPG445B	15.65 ± 0.05	14.82 ± 0.02	14.23 ± 0.05	13.54 ± 0.05	0.83 ± 0.06	...
KPG491A	16.34 ± 0.05	15.36 ± 0.02	14.69 ± 0.05	13.86 ± 0.05	0.98 ± 0.05	BS <sup>a</sup>
KPG491B	14.85 ± 0.05	13.92 ± 0.02	13.33 ± 0.05	12.65 ± 0.05	0.93 ± 0.05	...
KPG526A	13.36 ± 0.05	12.41 ± 0.02	11.75 ± 0.05	11.03 ± 0.05	0.95 ± 0.05	BS <sup>a</sup>
KPG526B	13.46 ± 0.05	12.43 ± 0.02	11.78 ± 0.05	11.03 ± 0.05	1.03 ± 0.05	BS <sup>a</sup>
KPG548A	12.95 ± 0.06	12.00 ± 0.03	11.36 ± 0.06	10.57 ± 0.05	0.95 ± 0.07	BS <sup>a</sup>
KPG548B	13.94 ± 0.06	12.90 ± 0.03	12.24 ± 0.06	11.36 ± 0.05	1.04 ± 0.07	BS <sup>a</sup>
KPG553A	14.73 ± 0.05	13.60 ± 0.02	12.93 ± 0.05	12.19 ± 0.05	1.13 ± 0.06	...
KPG553B	15.61 ± 0.06	14.58 ± 0.03	13.92 ± 0.05	13.12 ± 0.05	1.03 ± 0.07	BS <sup>a</sup>

<sup>a</sup>BS = Bright Star Close/Superposed to a Galaxy.

Following Paper I and Paper II, a comparison of our total *B*-band magnitudes and those available in the RC3 Catalogue (de Vaucouleurs et al. 1991) is shown in Figure 1. A typical displacement of 0.13 can be inferred from the data, consistent with our total error estimates. The only significant difference is found for KPG445B. Figure 8 shows some dwarf-like systems surrounding KPG445B. If light from these neighbors is not properly taken into account, it could be altering the magnitude estimate. Our estimate shows clearly that KPG445A is brighter than KPG445B, while RC3 reported similar magnitudes. Since our procedure is yielding a consistent magnitude estimate for KPG445A, we trust our estimate for KPG445B.

Sources to compare our photometry for mixed pairs in other bands than *B* are difficult to find. However, in Figure 2 we compare our results with other independent *BVRI* magnitude estimates, extracted mainly from Prugniel & Heraudeau (1998; and references therein). The scatter in Fig. 2 can

be explained by differences in the observing conditions and the corresponding zero point scales of the photometric systems involved.

### 3. RESULTS

#### 3.1. Integrated Magnitudes and Colors

The observed magnitudes and colors for individual galaxies in the sample are presented in Table 4. Entries are as follows: Column 1 gives the identification in Karachentsev's Catalogue, Columns 2 to 5 give the total magnitudes in *B*, *V*, *R*, and *I* bands, Column 6 gives the observed (*B* − *V*) color, and Column 7 gives some notes regarding the presence of bright stars nearby in the field.

The individual corrected magnitudes and colors are presented in Table 5. Entries are as follows: Column 1 gives the identification in Karachentsev Catalogue, Columns 2 to 5 give the total corrected magnitudes in *B*, *V*, *R*, and *I* bands, taking into account galactic blue absorptions from Schlegel et al. (1998), internal extinction from Tully et al. (1998)

TABLE 5  
CORRECTED MAGNITUDES AND COLOR INDICES

KPG	$B_o$	$V_o$	$R_o$	$I_o$	$(B - V)_o$	$M_{B_o}$	$(B - V)_T^o$	$M_B^o$
KPG339A	14.27±0.31	13.86±0.23	13.45±0.17	12.78±0.10	0.42±0.39	-20.67	0.48±0.06	-20.27
KPG339B	15.09±0.06	14.21±0.03	13.62±0.06	12.96±0.05	0.88±0.06	-19.82	0.92±0.06	-19.68
KPG353A	11.67±0.18	11.03±0.12	10.57±0.12	9.97±0.12	0.64±0.22	-19.72	0.66±0.14	-19.63
KPG353B	9.84±0.12	8.93±0.07	8.36±0.11	7.57±0.11	0.91±0.14	-21.02	0.93±0.14	-20.94
KPG393A	15.23±0.05	14.47±0.02	13.84±0.05	12.92±0.05	0.76±0.06	-19.91	0.78±0.06	-19.87
KPG393B	14.13±0.52	13.60±0.39	13.16±0.27	12.63±0.15	0.53±0.65	-21.01	0.59±0.06	-20.82
KPG394A	14.79±0.11	14.16±0.07	13.64±0.10	12.77±0.10	0.63±0.13	-17.57	0.63±0.13	-17.58
KPG394B	11.30±0.85	10.80±0.65	10.43±0.45	9.92±0.26	0.50±1.07	-21.24	0.60±0.13	-21.07
KPG408A	14.44±0.05	13.53±0.02	12.93±0.05	12.26±0.05	0.92±0.06	-19.23	0.92±0.06	-19.20
KPG408B	15.18±0.34	14.63±0.26	14.27±0.18	13.83±0.10	0.55±0.42	-18.46	0.56±0.06	-18.60
KPG445A	14.13±0.05	13.24±0.02	12.62±0.05	11.82±0.05	0.89±0.06	-21.42	0.94±0.06	-21.26
KPG445B	15.29±0.11	14.55±0.08	14.00±0.07	13.35±0.06	0.74±0.14	-20.06	0.75±0.06	-19.91
KPG491A	15.77±0.18	14.92±0.13	14.31±0.10	13.56±0.07	0.86±0.22	-19.89	0.85±0.06	-19.76
KPG491B	14.08±0.27	13.30±0.20	12.81±0.15	12.25±0.09	0.77±0.34	-21.58	0.81±0.06	-21.43
KPG526A	12.72±0.18	11.89±0.13	11.32±0.10	10.71±0.07	0.83±0.22	-20.29	0.83±0.06	-20.23
KPG526B	13.01±0.05	12.11±0.02	11.52±0.05	10.84±0.05	0.90±0.06	-20.05	0.90±0.06	-20.07
KPG548A	12.15±0.23	11.34±0.17	10.82±0.13	10.16±0.08	0.81±0.28	-21.60	0.82±0.07	-21.38
KPG548B	13.46±0.06	12.56±0.03	11.96±0.06	11.15±0.05	0.90±0.07	-20.07	0.91±0.07	-20.05
KPG553A	14.22±0.05	13.24±0.03	12.64±0.05	11.97±0.05	0.97±0.06	-19.83	0.97±0.07	-19.88
KPG553B	14.46±0.69	13.56±0.53	13.05±0.36	12.47±0.20	0.90±0.87	-19.67	0.87±0.07	-19.87

with coefficients taken from Verheijen (2001), and K-corrections interpolated from Frei & Gunn (1994). Column 6 gives the corresponding corrected  $(B - V)$  color. Column 7 gives the corresponding absolute blue magnitude, taking into account corrections in Column 2. Column 8 gives the corrected  $(B - V)_T^o$  color, according to RC3. Finally, Column 9 gives the blue absolute magnitude applying corrections from RC3. Notice that while the correction by internal extinction done in RC3 depends mainly on the morphological type T, we preferred a more physical correction proposed by Tully et al. (1998) where the internal extinction depends directly on the objects' total luminosity. Unfortunately, the large uncertainties in  $B_o$ ,  $V_o$ ,  $R_o$ , and  $I_o$  are due to the associated errors for the internal extinction coefficients taken from Verheijen (2001).

Our observations span a range (9.84–15.77) and (0.42–0.97) mag in  $B_o$  and  $(B - V)_T^o$ , respectively. The observed  $(B - V)$  range is comparable to our previous two sets of mixed pairs and other reported samples of interacting galaxies with similar observations from the literature.

### 3.2. Colors and Morphology

As shown in Papers I and II, the combination of  $B$ -band filtered images and geometric parameters estimated from the surface photometry analysis are a powerful technique both for morphological classification and for revealing fine structural details most likely related to galaxy encounters. To discuss the optical morphology and its relationship to the global photometric properties, the final results for each pair are presented in the form of a mosaic (cf. Figures 3 to 12). Each mosaic includes: (1) a  $B$ -band image, (2) a  $B$ -band filtered image, (3)  $BVRI$  surface brightness and color profiles, and (4) the corresponding geometric (radial  $\epsilon$ , PA and  $a_4/a$ ) profiles.

The isophotal shape parameter  $a_4/a$  has been introduced for the study of diskyness and boxiness in ellipticals and to investigate “the continuity” between the diskys Es and lenticulars. Although it may be senseless to study this parameter in late-type galaxies (the disk is certainly present and furthermore the evaluation of  $a_4/a$  is strongly perturbed by the presence of the arms and H II regions), it has been included in our mosaics because these profiles give us an excellent opportunity of comparing, qual-

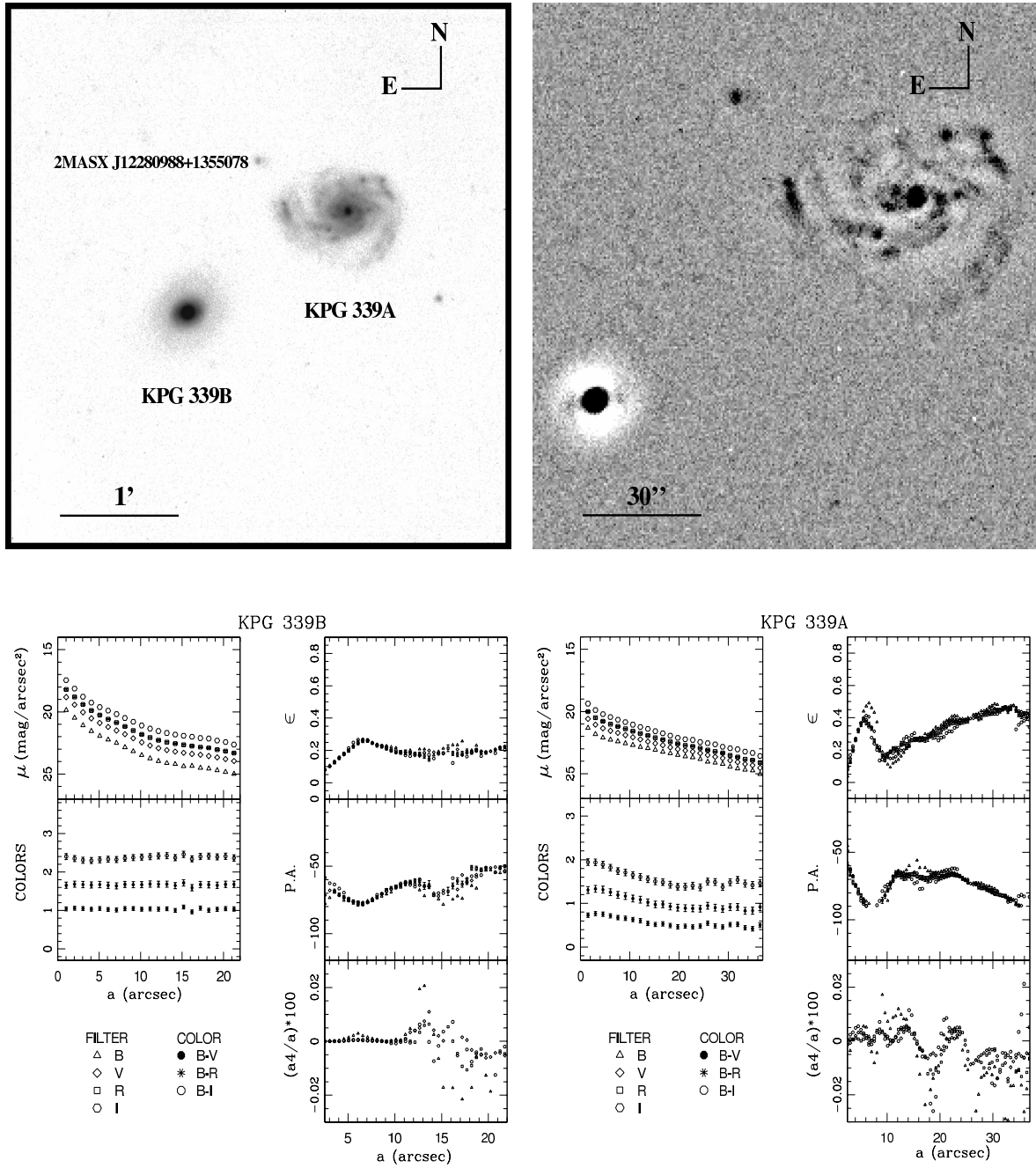


Fig. 3. KPG 339 Mosaic. Top left: *B*-band image. Top right: *B*-band filtered image. Bottom left: Surface brightness profile and geometric parameters for KPG 339A. Bottom right: Surface brightness profile and geometric parameters for KPG 339B.

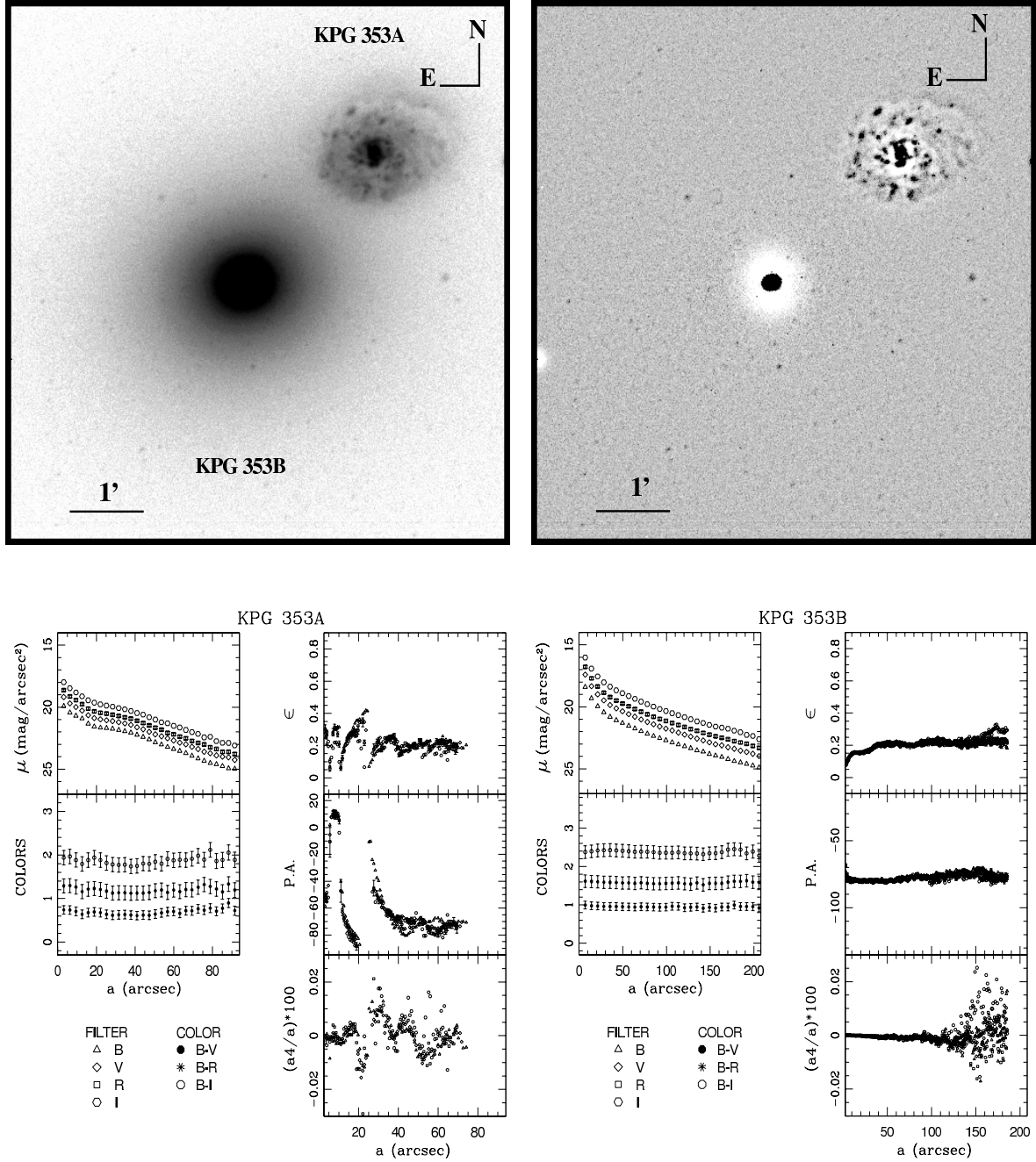


Fig. 4. KPG 353 Mosaic. Top left: *B*-band image. Top right: *B*-band filtered image. Bottom left: Surface brightness profile and geometric parameters for KPG 353A. Bottom right: Surface brightness profile and geometric parameters for KPG 353B.

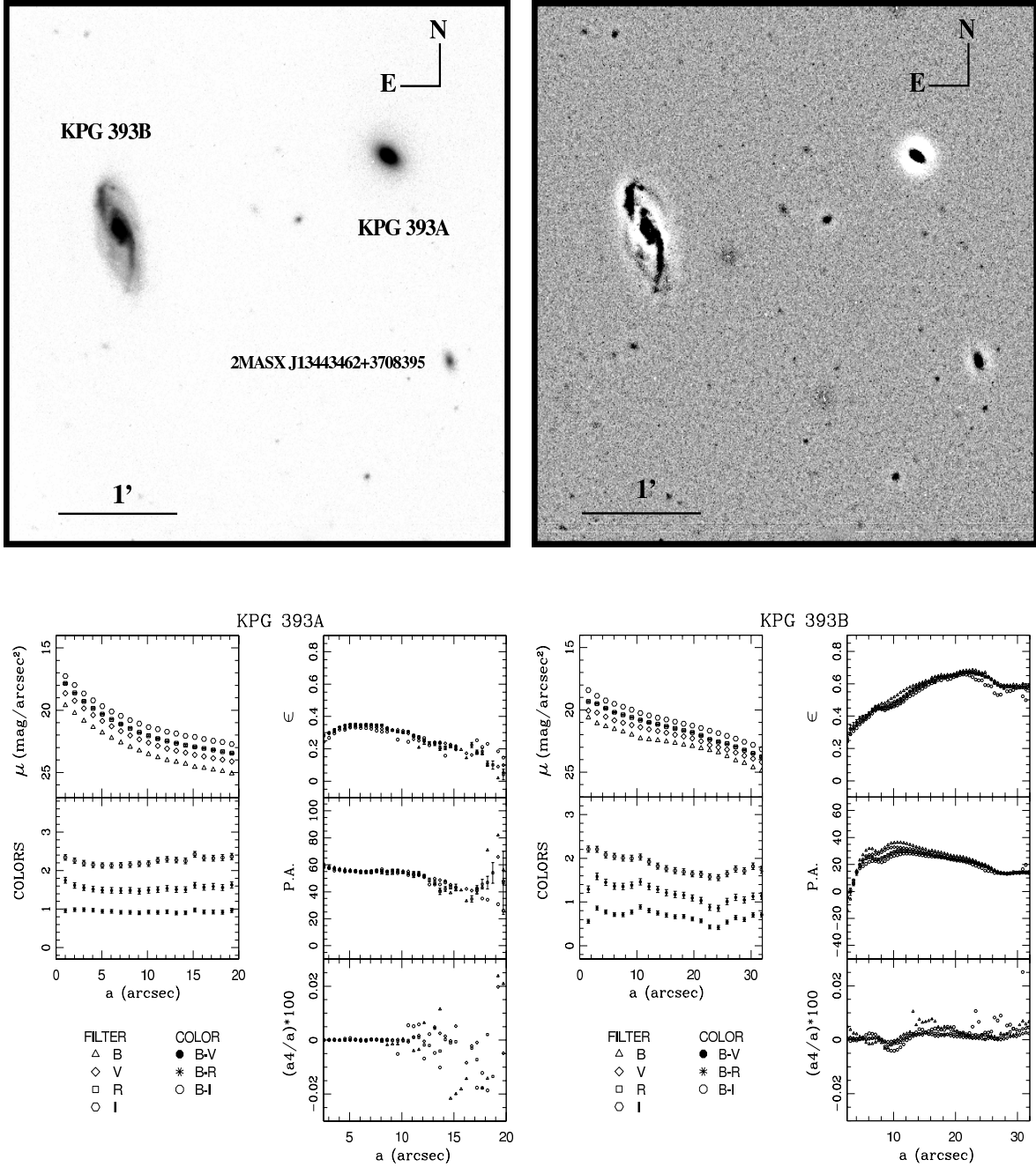


Fig. 5. KPG 393 Mosaic. Top left: *B*-band image. Top right: *B*-band filtered image. Bottom left: Surface brightness profile and geometric parameters for KPG393 A. Bottom right: Surface brightness profile and geometric parameters for KPG 393B.

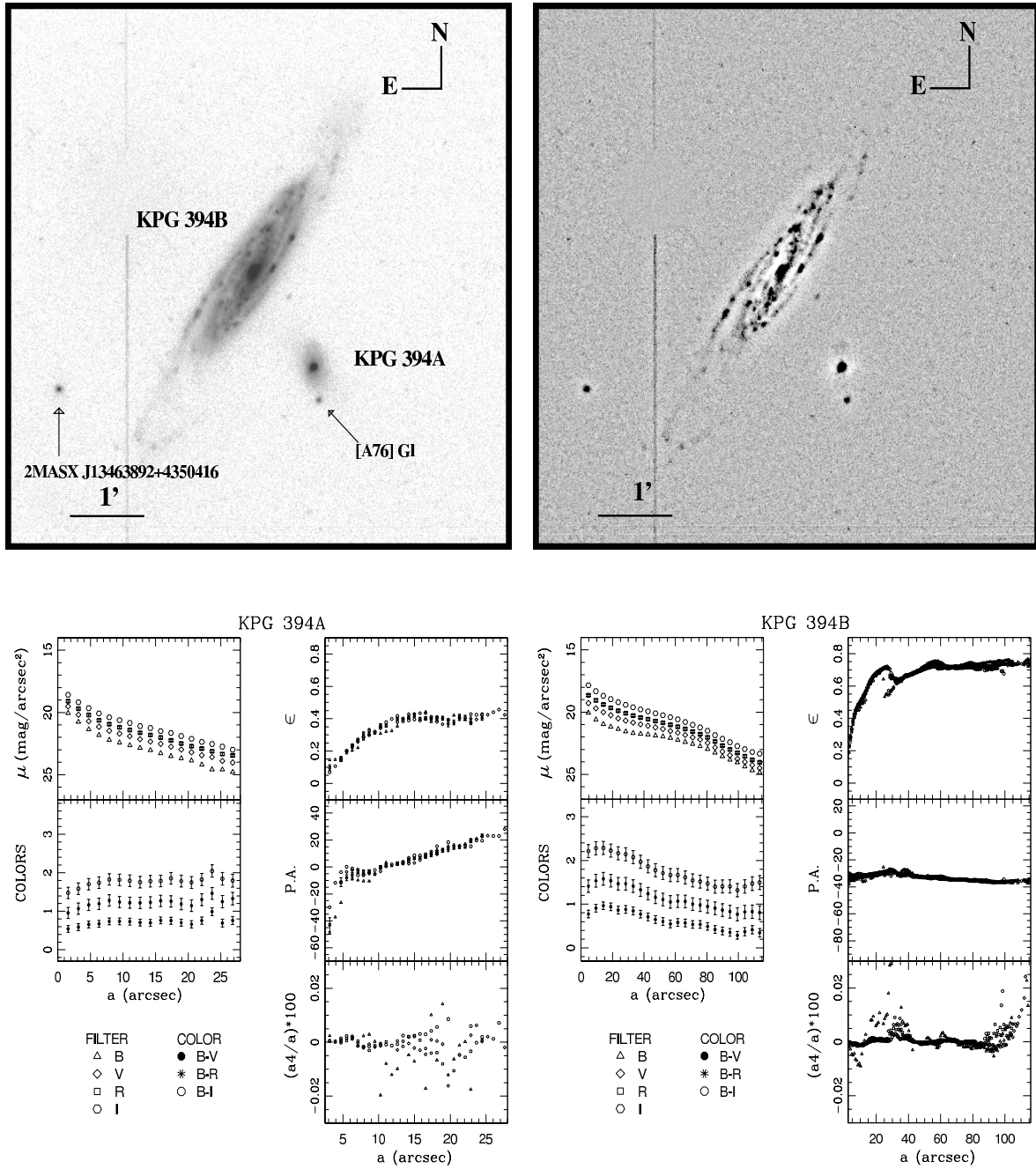


Fig. 6. KPG 394 Mosaic. Top left: *B*-band image. Top right: *B*-band filtered image. Bottom left: Surface brightness profile and geometric parameters for KPG 394A. Bottom right: Surface brightness profile and geometric parameters for KPG 394B.

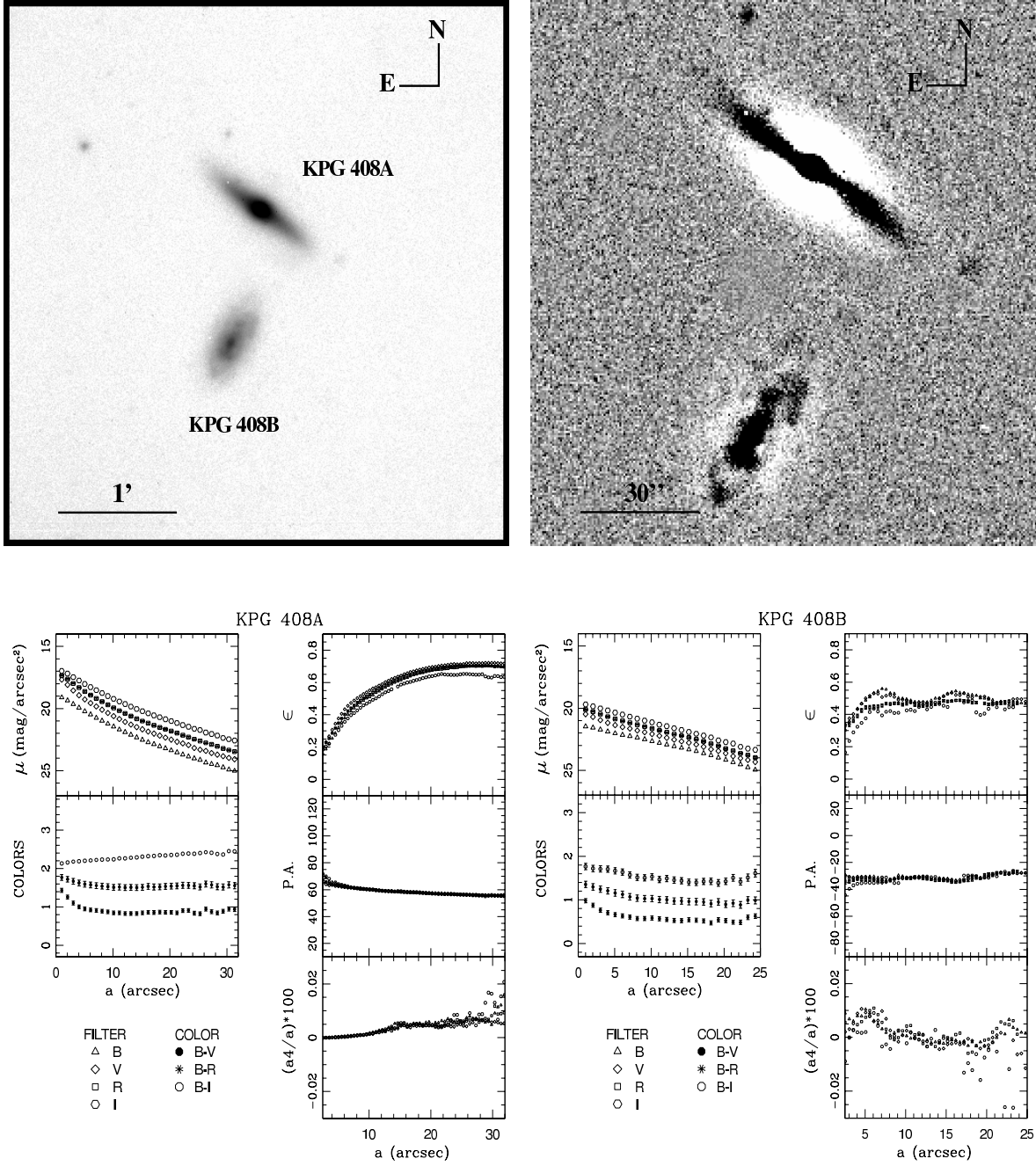


Fig. 7. KPG 408 Mosaic. Top left: *B*-band image. Top right: *B*-band filtered image. Bottom left: Surface brightness profile and geometric parameters for KPG 408A. Bottom right: Surface brightness profile and geometric parameters for KPG 408B.

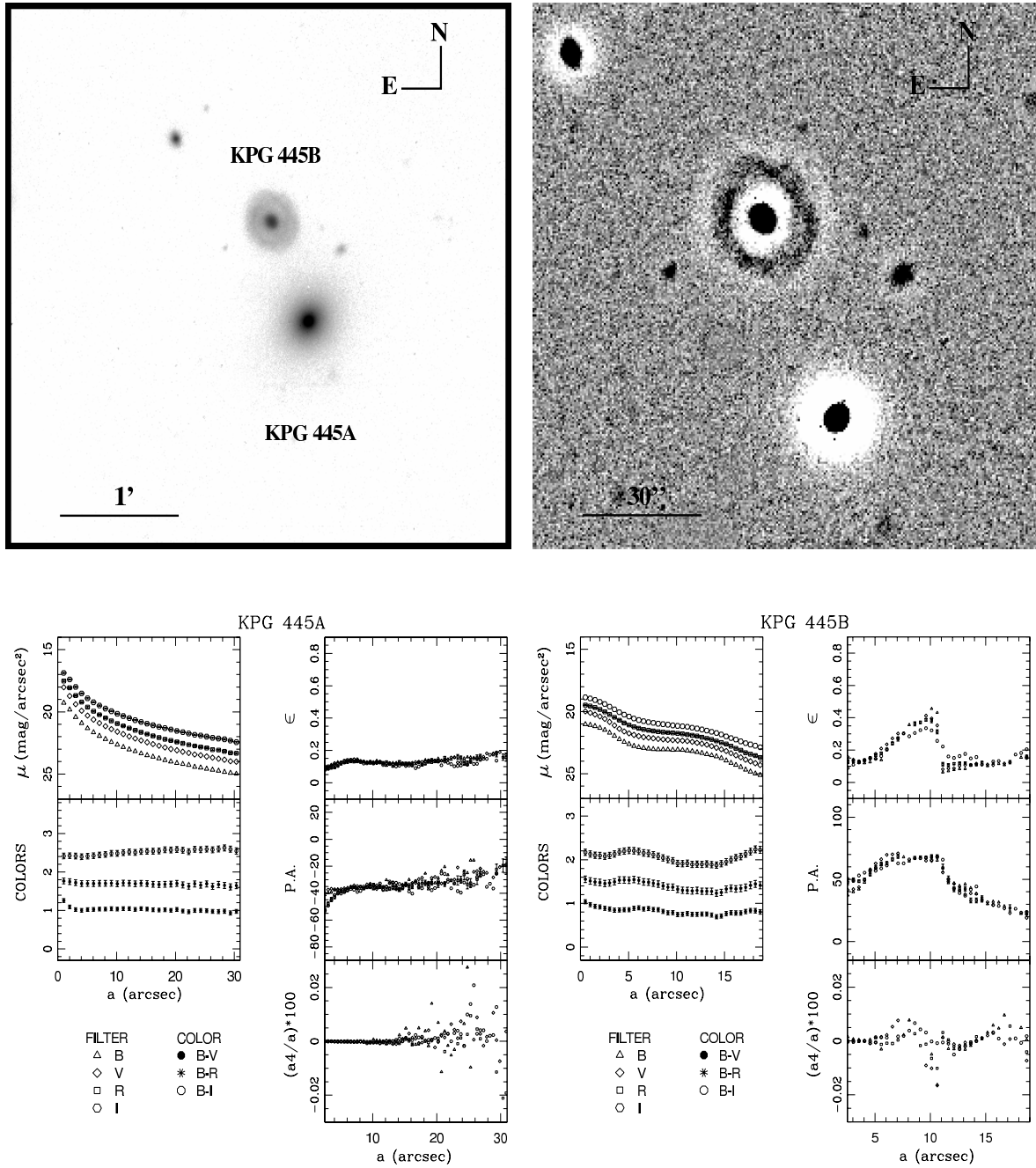


Fig. 8. KPG 445 Mosaic. Top left: *B*-band image. Top right: *B*-band filtered image. Bottom left: Surface brightness profile and geometric parameters for KPG 445A. Bottom right: Surface brightness profile and geometric parameters for KPG 445B.



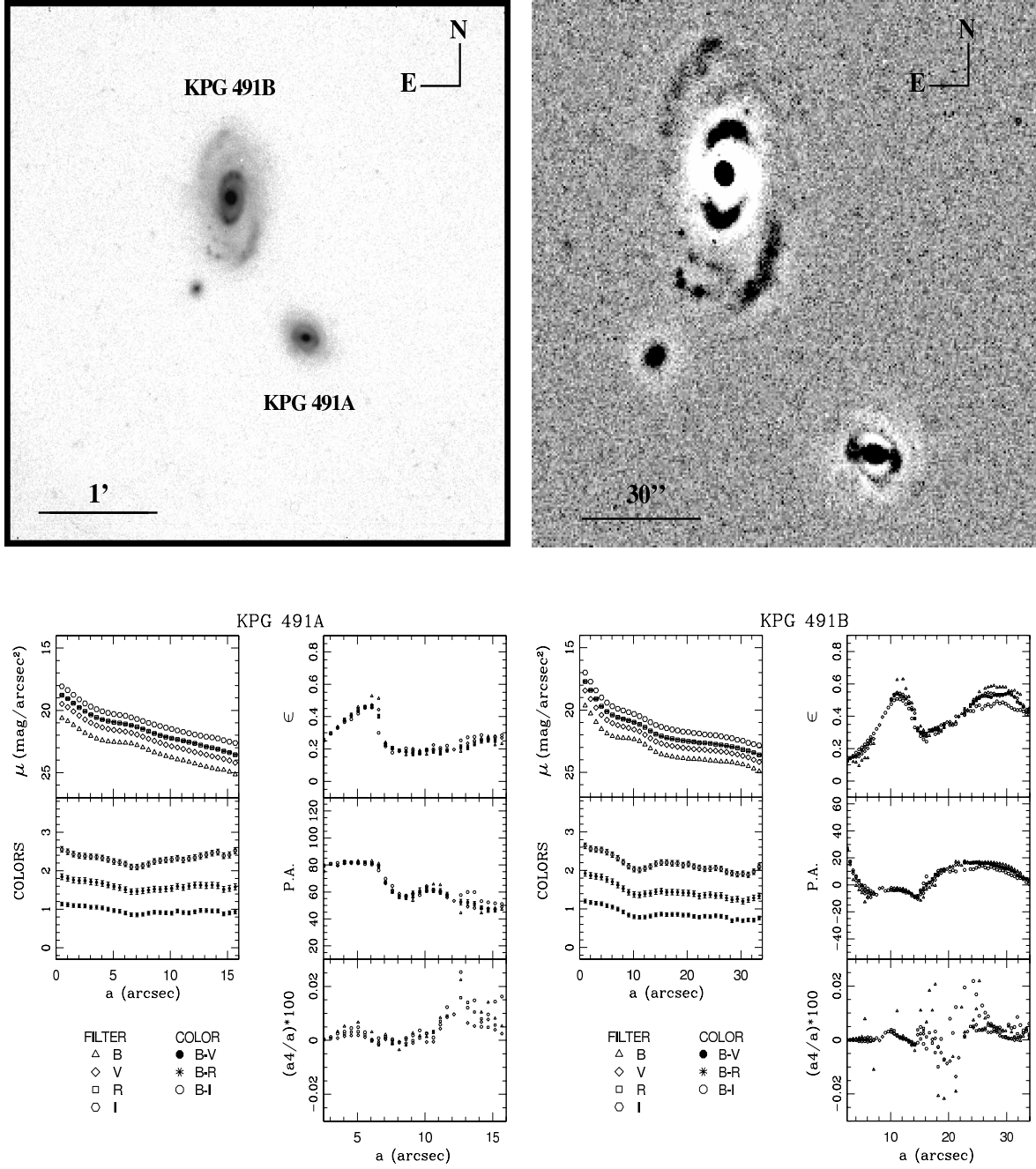


Fig. 9. KPG 491 Mosaic. Top left:  $B$ -band image. Top right:  $B$ -band filtered image. Bottom left: Surface brightness profile and geometric parameters for KPG 491A. Bottom right: Surface brightness profile and geometric parameters for KPG 491B.

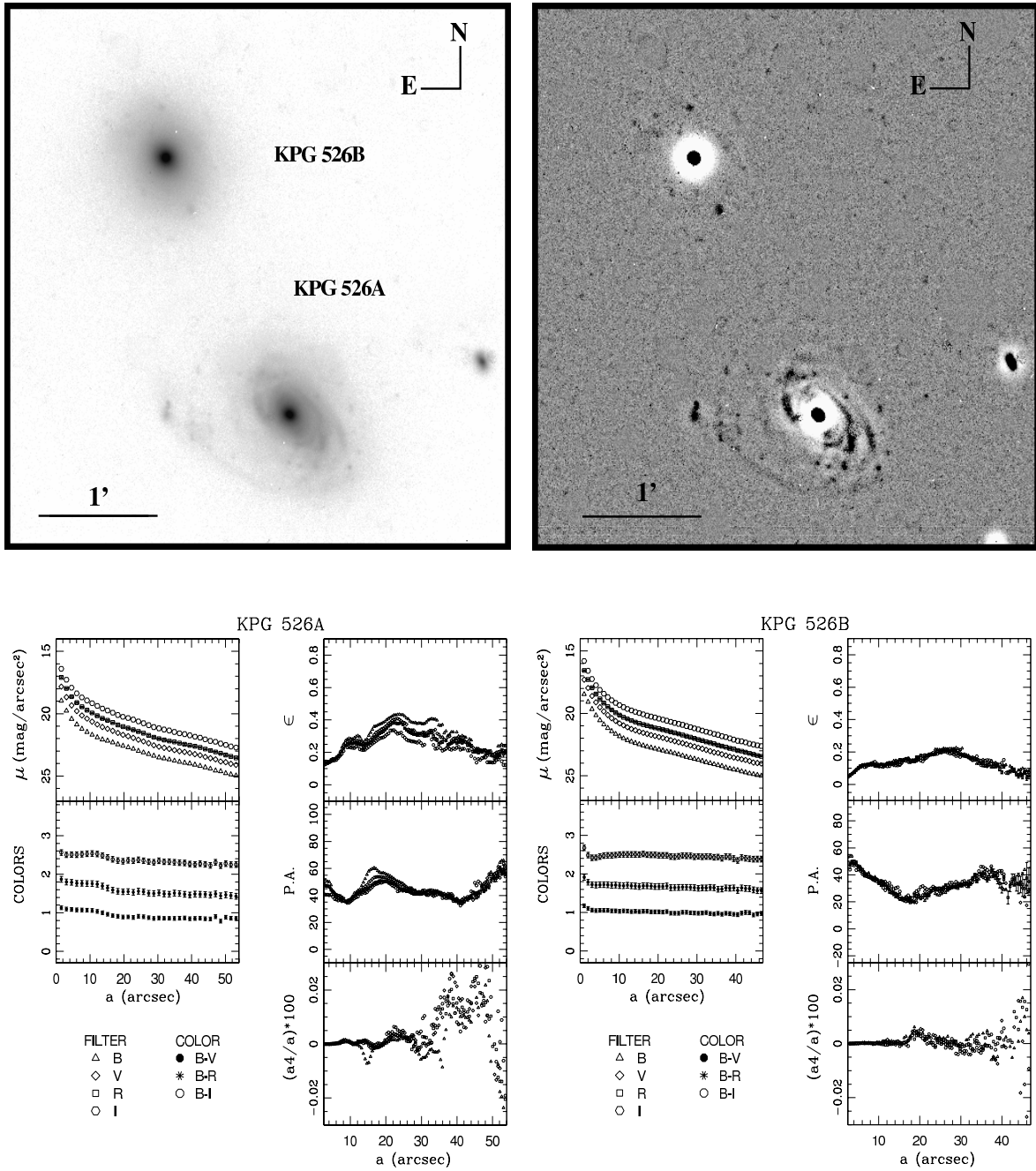


Fig. 10. KPG 526 Mosaic. Top left:  $B$ -band image. Top right:  $B$ -band filtered image. Bottom left: Surface brightness profile and geometric parameters for KPG 526A. Bottom right: Surface brightness profile and geometric parameters for KPG 526B.

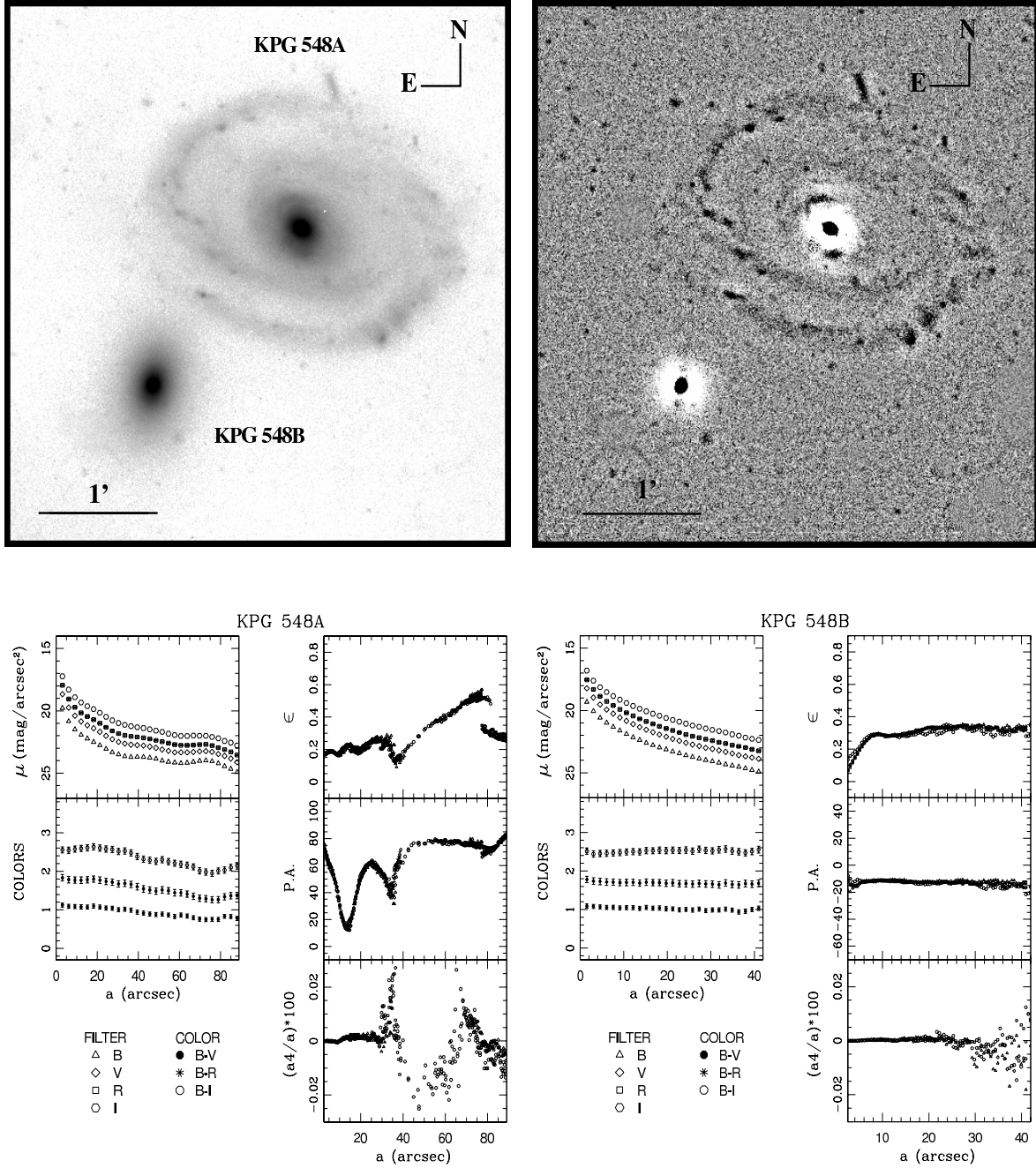


Fig. 11. KPG 548 Mosaic. Top left: *B*-band image. Top right: *B*-band filtered image. Bottom left: Surface brightness profile and geometric parameters for KPG 548A. Bottom right: Surface brightness profile and geometric parameters for KPG 548B.

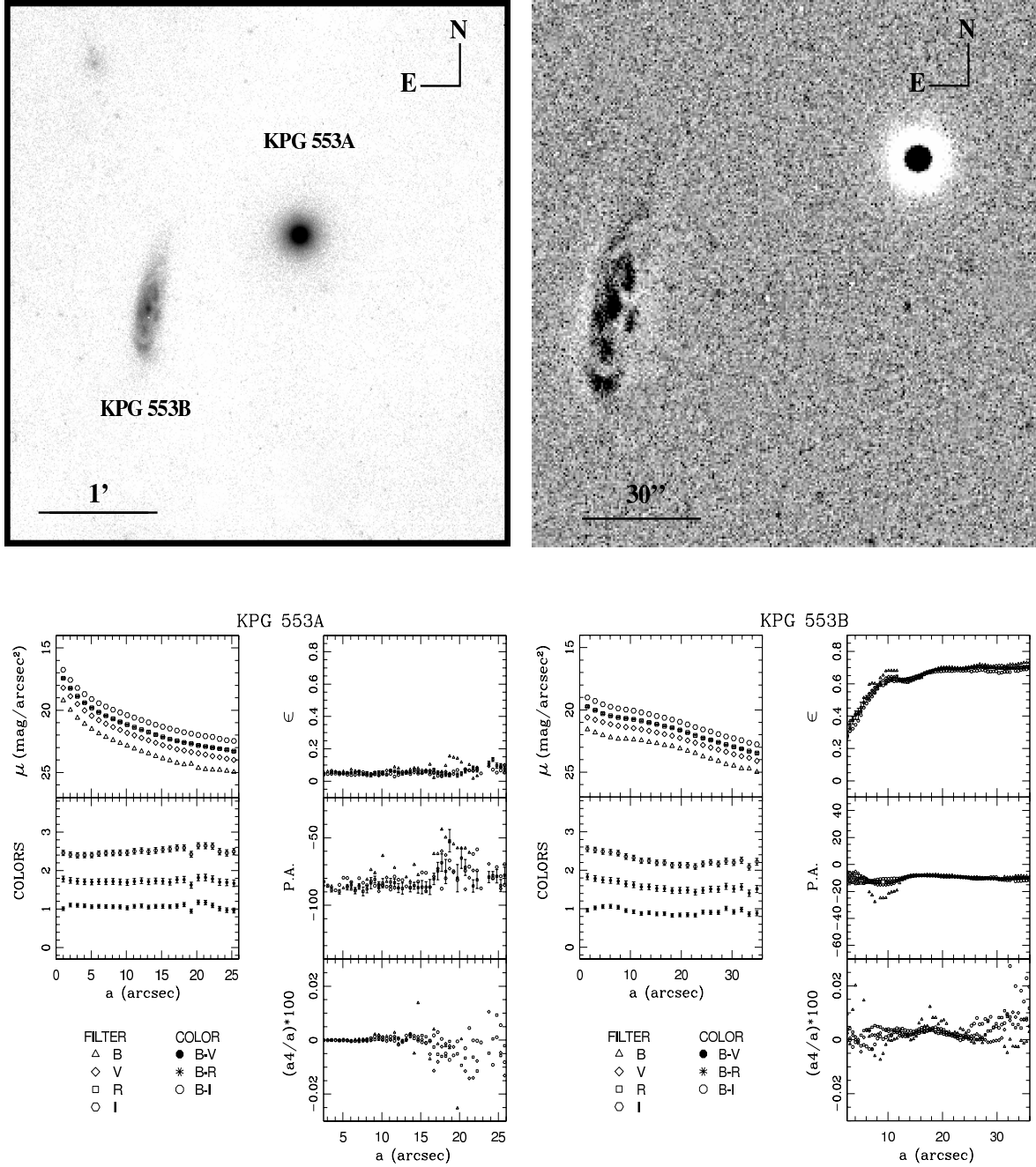


Fig. 12. KPG 553 Mosaic. Top left: *B*-band image. Top right: *B*-band filtered image. Bottom left: Surface brightness profile and geometric parameters for KPG 553A. Bottom right: Surface brightness profile and geometric parameters for KPG 553B.

itatively and quantitatively, the importance of disk and boxy structures in the E/S0 components of our sample of mixed pairs of galaxies.

We have carried out: (1) a reclassification of the previous POSS/LEDA Hubble morphology and (2) a classification of the spiral arm morphology as suggested by Elmegreen & Elmegreen (1982) (hereafter EE class), when possible. The discussion of morphological types also uses the information on the estimated mean colors  $(B - V)_T^0$ . Median integrated total  $(B - V)$  colors of galaxies according to morphological class are given by Roberts & Haynes (1994).

It is important to notice that Karachentsev pairs were selected according to a definite isolation criteria that does not allow other similar-sized galaxies to be found within the close neighborhood of a candidate pair. That is basically the case within the nominal field ( $6.7' \times 6.7'$  and  $4.3' \times 4.3'$ ) of our images. However, we also searched for radial velocity information for some small-sized galaxies detected in the close vicinity of the pairs and for other galaxies found when the field of view is increased. The information has been obtained from the Hyperleda database within fields of view of different angular sizes. Hyperleda uses a criterium to assign galaxies to a group and based on that, we comment about any possible belonging of our pairs to a group or higher order system. This is an important aspect that needs to be addressed in order to understand the pairs evolution.

The KPG employed an isolation criterion that requires

$$x_{ji}/x_{12} \geq \chi a_i/a_j; \quad j = 1, 2,$$

and

$$\xi a_j \leq a_i \leq \lambda a_j; \quad j = 1, 2,$$

where  $x_{ij}$  is the separation between the  $j$ th component and the nearest neighbor galaxy,  $x_{12}$  is the separation of the pair components, and  $a$  is the major-axis diameter of the respective galaxies. The isolation criterion identifies the least isolated pairs with coefficients:

$$\chi = 5, \xi = 0.5, \lambda = 4.$$

This means that identically sized galaxies in a pair cannot have neighbors closer than 5 times the distance between the components of the pair. The isolation criterion increases the probability that the observed pairs are physical binaries, rather than chance projections. Radial velocity measures exist for all KPG pairs, which allow the identification of discordant pairs ( $\sim 10\%$  of the KPG). The KPG provides

a well-defined sample without obvious morphological or luminosity biases (Teerikorpi 2001).

In addition, we produce red-green-blue (RGB) composite images of all our fields in order to analyze the color structure of each galaxy and test their degree of isolation. We follow the method proposed by Lupton et al. (2004), using our broadband  $R$ ,  $V$ , and  $B$  images. Additionally, our candidates for tidal dwarf galaxies were identified using simple criteria: they are located close to the end of spiral arms and have similar colors (Bournaud et al. 2004).

For a more detailed explanation about our morphological evaluation criteria see Paper I and II.

### 3.3. Comments on Individual Objects

**KPG 339.** This is an isolated system. We see only two small companions in the observed field: 2MASX J12280988+1355078 at  $53''$  to the north-east (NE) of KPG 339A, and an unidentified object at  $1'$  to the south-west (SW) of KPG 339A. In both cases, we do not have information on redshift; however their color  $(B - V) > 1.5$  suggests that these objects are foreground galaxies. **Component A:** this is a spiral galaxy with a multi-armed non-symmetric pattern. The presence of strong H II regions along the arms dominates the geometric and color profiles. The shape of the arms is less wound at the edge, probably due to tidal effects. Our  $\mu$  profiles show a very small bulge ( $a \leq 5''$ ) visible in the images. We classify this galaxy as a Scd pec; however, the total  $(B - V)_T^0$  color is more representative of Sm/Im types. Our EE classification is 2. **Component B:** the  $\epsilon$  and PA profiles suggest the presence of a bar (within  $a \sim 10''$ ) and a two-fold precessing structure, perhaps a tidally induced spiral pattern. The bar and an external disk are visible in the  $\mu$  profiles. We classify this galaxy as a SB0 pec, in agreement with their total  $(B - V)_T^0$  color.

**KPG 353.** Due to their large angular size, this pair is apparently isolated; however, the system is in the outskirts of the Virgo cluster. The nearest cluster companion of comparable angular size ( $r \sim 1'$ ) is NGC 4638, at  $13.7'$  to the SW of KPG 353A. **A:** this is a non-symmetric flocculent spiral where global appearance is dominated by numerous H II regions. The shape of geometric profiles within  $20''$  suggests the presence of a barred structure. An outer dust lane to the north delineates an external arm (probably of tidal origin). We classify this galaxy as a SAB(rs)cd pec; however, the total  $(B - V)_T^0$  color is more representative of Sab/Sb types. In this case, the presence of an important dusty component can be responsible for its reddening. Our EE classifica-

tion is 2. **B**: the geometric profiles are consistent with a typical elliptical galaxy; however, the  $\mu$  profiles show the presence of an extended envelope resembling a face-on disk in the external region. We classify this galaxy as an E2 pec, in agreement with the total  $(B - V)_T^0$  color. An iterative masking procedure was applied to eliminate light contamination from one component into the other.

**KPG 393.** Our images show some small red galaxies in the field  $[(B - V) > 1.5]$ , apparently associated with a foreground unknown cluster observed in a wider angle search ( $15' \times 15'$ ) to the SW of this pair. Unfortunately, redshift data are not available for these objects. The only galaxy identified is 2MASX J13443462+3708395 (at  $1.7'$  to the SW of KPG 393A); the color  $(B - V) = 0.9$  is similar to the color of the members of KPG 393. **A**: our  $\mu$  profiles are consistent with an elliptical galaxy plus an external envelope (see the dispersion at the edge of the galaxy in the geometric profiles for  $a > 11''$ ). We classify this galaxy as an E(2-3) pec; however, the total  $(B - V)_T^0$  color is more representative of S0a/Sa types. **B**: we observe two prominent and blue symmetric arms delineated by star formation regions  $[(B - V) = 0.42]$ , with faint extensions on both sides resembling a outer pseudo-ring. Our images show an inner ring-like structure generated by the winding of the arms ( $a \sim 8''$ ), and a dust lane crossing the eastern arm. The intense star formation in the arms is probably tidally induced by the interaction with the elliptical companion. We classify this galaxy as an S(r)c pec; however, the total  $(B - V)_T^0$  color is more representative of Sbc/Sc types. The presence of strong dust lanes may be contributing to its reddening. Our EE classification is 11.

**KPG 394.** This is by far one of the most hierarchical and isolated pairs in our sample. The observed blue colors in both components suggest mutually induced star formation. We identify only two small objects projected in the field: [A76]G1 (a quasar with  $V_{rad} = 25872 \text{ km s}^{-1}$  at  $25''$  of the center of KPG 394A to the SW; see Arp 1976), and 2MASX J13463892+4350416 (a galaxy with  $V_{rad} = 29398 \text{ km s}^{-1}$  at  $3.2'$  to the SE of KPG 339B). **A**: Domingue et al. (2003) report an extended  $H_\alpha$  emission in the center of this galaxy, consistent with our color profiles which show a blue compact bulge ( $a \leq 8''$ ). An external disk is visible in the  $\mu$  profiles. The observed monotonic twisting towards the companion may be produced by strong tidal forces. We classify this galaxy as a S0 pec; however, the total  $(B - V)_T^0$  color is more representative of Sab/Sb types. **B**: this is a highly inclined spiral with a flocculent morphol-

ogy. Strong star formation regions appear delineating multiple arms. A small bulge ( $a \leq 10''$ ) is visible in our  $B$ -band image. We infer the presence of a bar from the  $\epsilon$  and PA profiles in the inner  $35''$ . The  $B$ -band filtered image shows two faint extensions at the edge of the spiral arms ( $a > 1.5'$ ), probably induced by the interaction. We classify this galaxy as a SBcd pec, in agreement with the total  $(B - V)_T^0$  color. Our EE classification is 3. Our surface brightness, color, and geometric profiles are in concordance with the values reported by Rampazzo et al. (1995).

**KPG 408.** This is a very isolated pair. Our images show three small companions projected in the field without identification or redshift data. The nearest two of them have similar colors  $[(B - V) \sim 0.95]$  and are apparently associated to KPG 408A. In our  $B$ -band filtered image, the first is located at  $38''$  of the center of KPG 408A to the NE, and the other is located at  $48''$  to the SW; both are candidate tidal dwarf galaxies. **A**: this is an edge-on lenticular galaxy. Our PA profiles show a monotonic isophotal twist towards the companion, may be produced by strong tidal forces. We classify this galaxy as an S0 pec, in agreement with the total  $(B - V)_T^0$  color. **B**: the galaxy shows a complex morphology. We observe two disrupted blue arms with several star formation regions, probably induced by the interaction. A faint disk-like pseudo-ring in the inner region ( $a \sim 7''$ ), and two faint opposite north-south outer extensions ( $a \sim 16''$ ) are visible in our  $B$ -band filtered image. We classify this galaxy as an S(rs)c pec, in agreement with the total  $(B - V)_T^0$  color.

**KPG 445.**  $B$ -band filtered image shows some small objects in the field with similar colors to the members of this pair  $[(B - V) = 0.8 - 1.0]$ , suggesting a possible association with the system. The brightest of them is located at  $65''$  of the center of KPG 445B to the NE, while a nearer and less luminous object is located at  $38''$  of the center of KPG 445A to the NNW. Unfortunately, no identifications or redshift data are available for these objects. **A**: the dispersion in the geometric profiles is due to the symmetric structure of this galaxy. Our  $\mu$  profiles show the presence of an extended envelope. A low brightness structure, observed at  $29''$  of the center of KPG 445A in the SSW direction, is visible in our  $B$ -band image. The external isophotes not show clear evidence of disk-like or boxy structure. We classify this galaxy as an E2 pec, in agreement with the total  $(B - V)_T^0$  color. **B**: our images show two symmetric arms forming an external pseudo-ring structure ( $10'' \leq a \leq 15''$ ). We do not detect typical star formation regions commonly found in the arms of normal spirals; how-

ever, the ring appears on average bluer than the disk [ $(B - V)_T^0(\text{disk}) \simeq 0.76$ ,  $(B - V)_T^0(\text{ring}) \simeq 0.71$ ], in agreement with Reduzzi & Rampazzo (1996). A bar can be inferred from the  $\epsilon$  and PA profiles for  $a \leq 10''$ . We classify this galaxy as an SBab pec, in agreement with the total  $(B - V)_T^0$  color. Our EE classification is 8.

**KPG 491.** This isolated (S+S) system was misclassified as a mixed pair. Other galaxies with comparable angular sizes are not observed in a wider angle search ( $30' \times 30'$ ). Our images show only an unidentified small object in the field with similar colors to the members of this pair [ $(B - V) \sim 0.95$ ], possibly associated with the system. **A:** originally classified as an E, this spiral galaxy shows a well defined ring ( $8'' \leq a \leq 12''$ ), and a prominent bar ( $a \leq 8''$ ). The ring is mainly homogeneous; however, at the opposite edge of the bar we observe two prominent H II regions. A faint extension (similar to a disrupted arm) is also visible to the south of the ring. The total  $(B - V)_T^0$  color of this object is more representative of S0/S0a types. Additionally, the color profiles suggest the presence of a dusty extended component. We classify this galaxy as an SB(r)ab pec. **B:** our  $\mu$  and color profiles show a very luminous and red central region ( $a \leq 12''$ ) dominated by a bright bulge and two prominent symmetric inner arms forming a ring structure at  $6'' \leq a \leq 12''$ . The external arms are delineated by strong star forming regions. We classify this galaxy as an S(r)bc pec; however, the total  $(B - V)_T^0$  color is more representative of S0a/Sa types. Our EE classification is 11.

**KPG 526.** An unidentified object was detected in the field at  $1.7'$  to the west of KPG 526A. Its colors suggest a possible association with the system [ $(B - V) \sim 0.93$ ]. **A:** this is a multiple arm disk galaxy with notorious signs of interaction. Numerous star formation regions dominate the morphology of this object, as can be seen in our  $B$ -band filtered image. The geometric profiles show an important dispersion due to the asymmetric spiral structure; the shape of the external arms is less definite. Our images show a low brightness condensation at the top edge of the southern long arm ( $a \sim 62''$  to the east). It is a candidate tidal dwarf galaxy. The small bulge ( $a \leq 10''$ ) is surrounded by internal arms forming a pseudo-ring structure ( $a = 18'' - 24''$ ). We classify this galaxy as a S(r)bc pec; however, the total  $(B - V)_T^0$  color is more representative of S0/S0a types. The presence of strong dust lanes contribute to its reddening. Our EE classification is 4. **B:** this is a face-on lenticular galaxy. Our  $\mu$  profiles show a compact bulge ( $a \leq 10''$ ) and a large disk. The

dispersion in  $\epsilon$  and PA profiles confirm the presence of faint underlying structures on the disk, barely appreciated in our  $B$ -band filtered image. We classify this galaxy as an S0 pec, in agreement with the total  $(B - V)_T^0$  color.

**KPG 548.** A wide angle view ( $40' \times 40'$ ) shows this pair as the brighter member of the higher order aggregate UZC-CG 272 (Ramella et al. 2002). The nearest companion of comparable angular size ( $r \sim 17''$ ) is NGC 6961, at  $3.3'$  to the NW of KPG 548A. **A:** the presence of large H II regions dominate the shape of the geometric profiles and delineate two principal low surface brightness arms that appear forming a pseudo-ring in the inner region ( $25'' \leq a \leq 40''$ ). Rampazzo et al. (1995) suggested a weak bar in the central region of this galaxy ( $a \leq 20''$ ); however, the observed shape of the  $\epsilon$  and PA profiles does not show evidence of this structure. Our images show a peculiar elongated object located at  $72''$  of the center to the north. Its color [ $(B - V) \sim 0.8$ ] suggests a possible association with the north-east arm. This is another candidate tidal dwarf galaxy. We classify this galaxy as an S(r)ab pec; however, the total  $(B - V)_T^0$  color is more representative of S0/S0a types. Our EE classification is 11. **B:** the  $\mu$  profiles suggest the presence of an extended envelope in this elliptical (notice the dispersion at the edge of the galaxy in the geometric profiles for  $a > 28''$ ). Our surface brightness, color, and geometric profiles are in concordance with the values reported by Rampazzo et al. (1995). We classify this galaxy as an E3 pec, in agreement with the total  $(B - V)_T^0$  color.

**KPG 553.** Our  $B$ -band image shows the presence in the field of an unidentified object of very low surface brightness at  $2.2'$  to the NE of KPG 553A. Its colors suggest a possible association with this pair [ $(B - V) \sim 1.02$ ]. **A:** the  $\mu$  profiles show a classical elliptical galaxy; however, the external region ( $a > 21''$ ) shows a significative gradient to the blue in our color profiles, suggesting the presence of an external envelope. The notorious dispersion in the PA profiles is due to its low ellipticity. We classify this galaxy as E(0-1) pec, in agreement with the total  $(B - V)_T^0$  color. **B:** this is a very perturbed galaxy with a highly inclined and asymmetric disk, and a small bulge ( $a \leq 5''$ ). A faint filamentary extension (probably of tidal origin) can be seen to the north. We classify this galaxy as Scd pec; however, the total  $(B - V)_T^0$  color is more representative of E/S0 types. The  $B$ -band filtered image shows the presence of several dust lanes that produce its disrupted appearance and contribute to its reddening.

## 4. DISCUSSION

In order to explain the origin of mixed pairs and their morphology, we consider: (a) the degree of isolation, (b) the presence of substructures in both components, and (c) the fraction of true (E+S) pairs.

The environmental density plays an important role in the evolution of isolated mixed pairs. The picture of hierarchical galaxy formation (so-called ‘bottom-up universe’) assumes longer assembly timescales for the more massive galaxies with merging of galaxies and the infall of new cold gas from a galaxy’s halo being the main drivers (see Christlein & Zabludoff 2005 and references therein). In this scenario, interactions are adequate to induce star formation and to stimulate deviations from symmetry as evidenced by the presence of bridges, tails, bars and rings structures in the spiral component of mixed pairs, while the presence of shells, ripples and envelopes is presumably related to encounters and mergers in the elliptical component (Naab & Burkert 2003).

In the present sample, a high fraction of pairs (70%) show the presence of nearby faint companions; however, only a few objects have radial velocities to confirm their association. In other cases like KPG 353 and KPG 548 a wider viewing angle reveals that they are part of higher order systems.

For the late-type components, a candidate for tidally-generated spiral structure is KPG 445A. Other cases like KPG 393B, KPG 394B and KPG 526A show evidence of faint outer spiral structure apparently as a continuation of a more definite inner spiral structure.

Following Elmegreen & Elmegreen (1982), we succeeded in classifying 8 spirals. Some of the spirals in this sample are nearly edge-on, strongly interacting or simply do not fit into the Elmegreen & Elmegreen classes. In some cases we observe enhanced spiral patterns, probably induced by the interaction. Notice that structures on the disk of KPG 393B, KPG408B, and KPG 553B are not clearly seen due to inclination effects and the presence of strong dust lanes.

Contrary to the results in Paper II, an overrepresentation of types later than Sb is present: only 3 spirals of types earlier than Sb were found. Similarly, about 60% of the disk components show evidence of ringed structure, whereas 5 galaxies out of 20 (25%) show evidence of barred structure; two of them showing a flat color profile. Notice that only one is associated with spiral galaxies later than Sb.

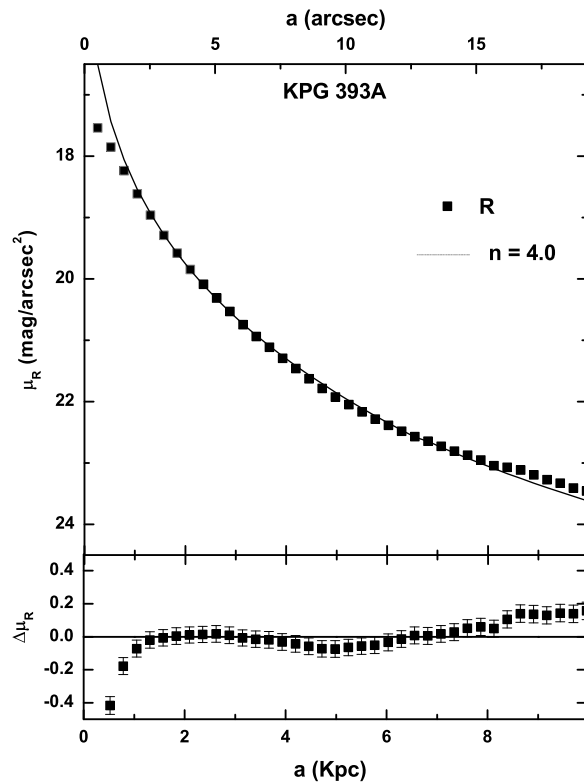


Fig. 13. Evidence of an external envelope in KPG 393A. Open squares:  $R$ -band surface brightness profile. Solid line: our best fit using a Sérsic model with  $n = 4.0$ . The difference between model and data from  $\mu_R > 23$  mag/arcsec<sup>2</sup> suggest the presence of an external envelope.

On the other hand, for the early-type components, we found evidence of twisting in KPG 339B, KPG 393A, KPG 394A, KPG 408A, KPG 445A, and KPG 526B. Additionally, KPG 339B shows signals of a bar structure and hints of induced arms.

In most of the cases it is not easy to identify the presence of envelopes in elliptical galaxies. In Figure 13 we approximate the  $R$ -band surface brightness profile of KPG 393A to the  $r^{1/n}$  law introduced by Sérsic (1968), following the procedure proposed by Trujillo et al. (2004). The best fit was found when we consider only one component with  $n = 4.0$ , the traditional de Vaucouleurs (1958)  $r^{1/4}$  profile. However, the difference between model and data from  $\mu_R > 23$  mag/arcsec<sup>2</sup> suggest the presence of an external envelope in this object. The surface brightness profiles of KPG 353B, KPG 445A, KPG 548B, and KPG 553A show a similar behavior.

A more extensive analysis, including surface brightness fitting in the  $B$ ,  $V$ ,  $R$ , and  $I$  bands for all the objects in our sample, will be reported in a future work.



Finally, we found a 50% fraction of true (E+S) pairs in agreement with the results in Paper I and Paper II. The remaining objects include 4 lenticular-spiral (S0+S) systems and 1 spiral-spiral (S+S) system. Our results suggest that an important fraction of (E+S) pairs are a by-product of the secular evolution of pairs and groups.

#### 4.1. Color Diagram and Holmberg Effect

Three main factors that govern the color of a galaxy are: (1) the relative number of luminous blue stars (which in turn depends on the star-formation rate in the galaxy or on how long ago star formation terminated, as well as on the initial mass function); (2) the star chemical composition (the decisive factor for systems containing no young stars); (3) reddening produced by the interstellar matter in the galaxy. These factors are strongly influenced by interactions.

Holmberg (1958) suggested that there is a correlation between the integrated colors of pair members; this correlation is known as the “Holmberg Effect”. The Holmberg Effect has been interpreted as: (a) evidence that similar types of galaxies form together (morphological concordance), because local environment determines galaxy morphology. It might also reflect (b) synchronized star formation histories in the pair components, or (c) a combination of both (Kennicutt et al. 1987).

Similarly to Paper I and Paper II, we continue to analyze the evidence for a possible correlation between the colors of mixed pair components. After re-evaluating the morphological classification (see Paper I and Paper II), we compare in Figure 14 the  $(B - V)_T^0$  color indices of components in the present sample. The color index along the vertical axis refers to the late type component and that along the horizontal axis refers to the early type component in each pair. In order to reinforce any possible correlation, in addition to the data in the present sample the data from Paper I and from Paper II are also included.

In Paper II, we said that from the color diagram (Fig. 14) we found a trend indicating a possible Holmberg Effect. *This trend is not confirmed with the additional data of the present paper.* This finding is in agreement with the result of Reduzzi & Rampazzo (1996) who find a Holmberg Effect for (E+E) and (S+S) pairs but not for mixed pairs.

There is a group of galaxies whose color indices widen the scatter in Fig. 14 beyond any possible error. We have analyzed this subset of 8 mixed pairs composed by KPG 29, KPG 86, KPG 129, and KPG 162 from Paper I, KPG 392 from Paper II, and KPG

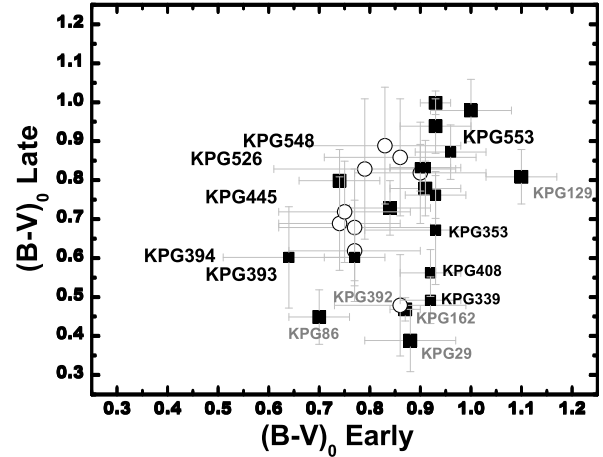


Fig. 14. Our color diagram:  $(B - V)_T^0$  early-type galaxy versus  $(B - V)_T^0$  late-type galaxy. Filled squares: Mixed pairs in this work. Open squares: Mixed pairs from Paper I. Open circles: Mixed pairs from Paper II.

339, KPG 353, and KPG 408 from Paper III (see Fig. 14), in order to see if they somehow constitute a particular sub-group of pairs related among them by a special property (e.g., morphology, starburst properties, separation, hierarchical pairs, radial velocities, etc.). The result is negative: they are an ensemble of pairs apparently non-related by any common property. As of now, from a combination of this and the previous reports, *we conclude that there is no clear evidence of a Holmberg effect in our sample of 31 mixed pairs.*

## 5. SUMMARY

Table 6 is a summary of the morphological features found in this work. Column 1 gives the pair catalogue number, Column 2 gives the Hubble Type as reported in NED, Column 3 gives the Hubble Type as estimated in this work, Column 4 gives the Elmegreen (EE) class, Column 5 indicates when other galaxies (dwarfs or galaxies of comparable size) are in the neighborhood of the pair, Column 6 indicates when a flat or positive gradient color profile is present, and finally Column 7 indicates the presence of rings, bars and knotty structures associated with star formation regions.

Three confirmed AGN were found in the literature: two LINERS (KPG 394B, Domingue et al. 2003; KPG 526A, Barth et al. 1997) and one radio galaxy (KPG 445A, Condon & Broderick 1988). Additionally, KPG 353B is a detected X-ray source (a possible AGN), whereas KPG 339A and KPG 548A were reported at a  $1\sigma$  level in Henriksen & Cousineau (1999). The presence of nuclear activity in galaxies

TABLE 6  
FINAL RESULTS FROM THIS STUDY

Name	Hubble Type(NED)	Hubble Type <sup>a</sup>	EE Class	Isolation	Profile	Notes
KPG 339A	Scd:	Scd pec	2	...		K, TA
KPG 339B	SB0?	SAB0 pec	...	...		B?, TA?
KPG 353A	SAB(rs)c	SAB(rs)cd pec	2	ACGC	F	B?, K, TA?
KPG 353B	E2 (X Ray source)	E2 pec	...	...		...
KPG 393A	E	E(2-3) pec	...	ADCG		...
KPG 393B	SB?	S(r)c pec	11	...		K, R, TA
KPG 394A	S0+:	S0 pec	...	...	+	...
KPG 394B	SAB(s)c: sp (LINER)	SBcd pec	3	...		B, K, TA
KPG 408A	S0/a	S0 pec	...	ADCG		...
KPG 408B	S?	S(rs)c pec	...	...		K, R?
KPG 445A	S0 (AGN Radio Galaxy)	E2 pec	...	ADCG		...
KPG 445B	S0?	SBab	8	...	F	B, R
KPG 491A	E	SB(r)ab pec	...	ADCG	F	B, K, R
KPG 491B	Sab	S(r)bc pec	11	...		K, R
KPG 526A	SAab: (LINER)	S(r)bc pec	4	ADCG		K, R, TA
KPG 526B	SA0+:	S0 pec	...	...		K?
KPG 548A	SAB(r)ab	S(r)ab pec	11	ADGC		K, R
KPG 548B	E+ pec:	E3 pec	...	ACGC	-	...
KPG 553A	E	E(0-1) pec	...	ADCG		...
KPG 553B	Scd:	Scd pec	...	...		K, TA?

<sup>a</sup>This work. NOTES TO TABLE: ADCG = Apparent Dwarf Companion Galaxy in the Field. ACGC = Apparent Companion Galaxy of Comparable size near. ACGC = Apparent Companion Galaxy of Comparable size near. F = Flat color profile. + or - = Positive or negative gradient in color profile. B = Bar. K = Knots. R = Ring. TA = Tidal Arms.

of mixed pairs (3/22 from Paper I, 3/20 from Paper II, and 3/20 in the present paper), along with the high percentage of AGNs with close neighbors are important signals of the AGN-interaction connection (cf. Dultzin-Hacyan et al. 1999). The number of true (E+S) pairs in our sample ( $\sim 50\%$ ), the presence of ellipticals with envelopes and the detected candidate tidal dwarfs around spirals are important evidence of a nurture scenario in this type of pairs.

A. F-B. acknowledges CONACyT for a scholarship. A. F-B., D. D-H., and M. R. acknowledges support through grants IN118601, IN100703, and IN120802, from DGAPA, PAPIIT, UNAM, and 2002-C01-40095 from CONACyT. Partial support for this work was provided by CONACyT grant 42810/A-1 to H. M. H-T. We have made use of NED and LEDA databases throughout this paper.

## REFERENCES

- Arp, H. 1976, *ApJ*, 210, L59  
Athanassoula, E., Makino, J., & Bosma, A. 1997, *MNRAS*, 286, 825  
Barnes, J. E., & Hernquist, L. 1992, *ARA&A*, 30, 705  
Barth, A. J., Reichert, G. A., Ho, L. C., Shields, J. C., Filippenko, A. V., & Puchnarewicz, E. M. 1997, *AJ*, 114, 2313  
Bournaud, F., Duc, P.-A., Amram, P., Combes, F., & Gach, J.-L. 2004, *A&A*, 425, 813  
Christlein, D., & Zabludoff, A. I. 2005, *ApJ*, 621, 201  
Condon, J. J., & Broderick, J. J. 1988, *AJ*, 96, 30  
de Vaucouleurs, G., de Vaucouleurs, A., Corwin, H. G., & Buta, R. 1991, *Third Reference Catalogue of Bright Galaxies (RC3)*, (New York: Springer-Verlag)  
de Vaucouleurs, G. 1958, *Ann. Astrophys.*, 11, 247  
Domingue, D. L., Sulentic, J. W., Xu, C., Mazzarella, J., Gao, Y., & Rampazzo, R. 2003, *AJ*, 125, 555  
Dultzin-Hacyan, D., Krongold, Y., Fuentes-Guridi, I., &

- Marzianni, P. 1999, *ApJ*, 513, L111
- Elmegreen, B. G., & Elmegreen, D. M. 1982, *MNRAS*, 201, 1021
- Franco-Balderas, A., Hernández-Toledo, H. M., Dultzin-Hacyan, D., & García-Ruiz, G. 2003, *A&A*, 406, 415
- Franco-Balderas, A., Hernández-Toledo, H. M., & Dultzin-Hacyan, D. 2004, *A&A*, 417, 411
- Frei, Z., & Gunn, J. E. 1994, *AJ*, 108, 1476
- Henriksen, M., & Cousineau, S. 1999, *ApJ*, 511, 595
- Holmberg, E. 1958, *Lund Medd. Astron. Obs. Ser. II*, 136, 1
- Karachentsev, I. D. 1972, *Catalogue of Isolated Pairs of Galaxies in the Northern Hemisphere*, *Comm. Spec. Ap. Obs.*, 7, 1
- Kennicutt, R. C., Roettiger, K. A., Keel, W. C., van der Hulst, J. M., & Hummel, E. 1987, *AJ*, 93, 1011
- Landolt, A. U. 1992, *AJ*, 104, 340
- Lupton, R., Blanton, M. R., Fekete, G., Hogg, D. W., O'Mullane, W., Szalay, A., & Wherry, N. 2004, *PASP*, 116, 133
- Mihos, J. Ch. 1995, *ApJ*, 438, 75
- Naab, T., & Burkert, A. 2003, *ApJ* 597, 893
- Prugniel, P., & Heraudeau, P. 1998, *A&AS*, 128, 299
- Ramella, M., Geller, M. J., Pisani, A., & Da Costa, L. N. 2002, *AJ*, 123, 2976
- Rampazzo, R., Reduzzi, L., Sulentic, J. W., & Madejsky, R. 1995, *A&AS*, 110, 131
- Rampazzo, R., & Sulentic, J. W. 1992, *A&A*, 259, 43
- Reduzzi, L., & Rampazzo, R. 1996, *A&AS*, 116, 515
- Roberts, M. S., & Haynes, M. P. 1994, *ARA&A*, 32, 115
- Sérsic, J. L. 1968, *Atlas de galaxias australes Cordoba: Observatorio Astronomico*
- Schlegel, D. J., Finkbeiner, D. P., Douglas, P., & Davis, M. 1998, *ApJ*, 500, 525
- Schweizer, F., & Seitzer, P. 1992, *AJ*, 104, 1039
- Teerikorpi, P. 2001, *A&A*, 371, 470
- Trujillo, I., Erwin, P., Ramos, A., & Graham, A. 2004, *AJ*, 127, 1917
- Tully, R. B., Pierce, M. J., Huang, Jia-Sheng, Saunders, W., Verheijen, M. A. W., & Witchalls, P. L. 1998, *AJ*, 115, 2264
- Verheijen, M. A. W. 2001, *ApJ*, 563, 694
- Wiren, S., Zheng, J.-Q., Valtonen, M. J. & Chermin, A. 1996, *AJ*, 111, 160